Published in final edited form as:
Dev Dyn. 2014 March ; 243(3): 381–392. doi:10.1002/dvdy.24078.

Irx4 identifies a chamber-specific cell population that contributes to ventricular myocardium development

Daryl O. Nelson, BS[1], **Dexter Jin, BS**[1], **Karen Downs, PhD**[1], **Timothy J. Kamp, MD/PhD**[2], and **Gary E. Lyons, PhD**[1,*]

[1]Department of Cell and Regenerative Biology, School of Medicine & Public Health, University of Wisconsin, Madison, WI 53706

[2]Department of Medicine, School of Medicine & Public Health, University of Wisconsin, Madison, WI 53706

Abstract

Background—The ventricular myocardium is the most prominent layer of the heart, and the most important for mediating cardiac physiology. Although the ventricular myocardium is critical for heart function, the cellular hierarchy responsible for ventricle-specific myocardium development remains unresolved.

Results—To determine the pattern and time course of ventricular myocardium development, we investigated IRX4 protein expression, which has not been previously reported. We identified $IRX4^+$ cells in the cardiac crescent, and these cells were positive for markers of the first- or second heart fields. From the onset of chamber formation, $IRX4^+$ cells were restricted to the ventricular myocardium. This expression pattern persisted into adulthood.

Interestingly, we observed that IRX4 exhibits developmentally-regulated dynamic intracellular localization. Throughout prenatal cardiogenesis, and up to postnatal day 4, IRX4 was detected in the cytoplasm of ventricular myocytes. However, between postnatal days 5-6, IRX4 translocated to the nucleus of ventricular myocytes.

Conclusions—Given the ventricle-specific expression of Irx4 in later stages of heart development, we hypothesize that $IRX4^+$ cells in the cardiac crescent represent the earliest cell population in the cellular hierarchy underlying ventricular myocardium development.

Keywords

cardiogenesis; differentiation; heart fields

Introduction

Cardiogenesis encompasses several morphological changes triggered by molecular pathways, which drive cell fates, all leading to the formation of a four-chambered heart

*Corresponding Author: Gary E. Lyons, PhD, Department of Cellular and Regenerative Biology, University of Wisconsin-Madison, 1300 University Ave., SMI Room 319, Madison, WI 53706, Phone: 608-262-2874, gelyons@facstaff.wisc.edu.

The authors have no conflicts of interest to disclose.

(Evans et al., 2010; Moorman et al., 2003; Solloway and Harvey, 2003). The heart is the first functional organ to arise during mammalian embryogenesis, and the process of cardiogenesis starts as early as embryonic day 7 (E7). Onset is signified by the presence of $Mesp1^{+}$ cardiac progenitors in the nascent cardiac mesoderm, which lies adjacent to the primitive streak mesoderm (Saga et al., 2000; Kitajima et al., 2000). Within 24 hours, the cardiac crescent is formed. This hallmark structure is comprised of cardiac progenitors that are segregated into two cell groups, termed the first- and second heart fields. The second heart field is recognized as being composed of progenitors derived from the splanchnic mesoderm, and located in the medial and posterior regions of the cardiac crescent (Liang et al., 2013; Dyer and Kirby, 2009; Vincent and Buckingham, 2010; Francou et al., 2013). Progenitors of both heart fields contribute to the development of a mature, functional heart.

The cardiac crescent fuses at the mid-line to form the linear heart tube at ~E8.5 (Vincent and Buckingham, 2010). Chamber formation ensues as the heart tube exhibits regionalization with the atrial precursor, inflow tract, located at the venous pole, and opposite of the outflow tract, which will give rise to the aorta. The most prominent region of the heart tube is the primitive ventricular chamber, which is medially located. The myocardium, unlike epi- and endocardial counterparts, is primarily comprised of myocytes. Myocyte phenotype is one of the primary factors that distinguish the atrial and ventricular myocardiums, and this manifests in the physiology of the heart chambers. Expression of chamber-specific myocyte markers, such as Myl2, the ventricular isoform of myosin light chain, confirms that cardiomyocyte differentiation has occurred. Non-rhythmic contraction of the heart tube confirms that myocytes, and the cardiac conduction system are immature (Kubalak et al., 1994). The heart chambers become more obvious following looping of the heart tube, as the inflow tract moves dorsally, and in the anterior direction to sit atop the common ventricle (E9-10).

Following looping of the heart tube, the common ventricular chamber undergoes septation, myocytes mature, and the cardiac conduction system develops (Anderson et al., 2003; Fishman et al., 2005). These developmental events are crucial for ventricular physiology; perturbation of these maturation processes can impair cardiac physiology. As medical interventions move toward gene and cell therapeutics to cure cardiogenic anomalies, it is important to understand the process of ventricular myocardium differentiation.

While the morphogenesis underlying heart chamber formation is well studied, the cellular hierarchy responsible for ventricular myocardium specification remains unresolved. In this study, we use an immunostaining approach to identify the onset of ventricular myocardium specification, and development during murine embryogenesis by assessing the spatiotemporal expression pattern of Iroquois related homeobox protein 4 (*Irx4*). *Irx4* is a member of the Iroquois homeobox gene family, which encodes transcription factors, all of which play a role in heart development and function (Kim et al., 2012; Christoffels et al., 2000b). Results of Irx4 mRNA detection assays (Bao et al., 1999; Bruneau et al., 2000) suggest that the Irx4 transcription factor is expressed in progenitors of the cardiac crescent at E7.5-8. Irx4 transcripts exhibit ventricular specificity at the nascent stages of chamber formation, as they have been detected in the primitive ventricular myocardium of the linear heart tube (Christoffels et al., 2000a). Irx4 transcripts remain restricted to the ventricular

myocardium in the developing, pre- and postnatal heart (Bruneau et al., 2001). Although previously published in situ hybridization data have established an expression pattern for Irx4, these data do not reveal much about the cells that are positive for this transcription factor. Using co-immunofluorescence, we show that IRX4 is present in cardiac-specific troponin T^+ (cTnT) myocytes in embryonic, and neonatal cardiac tissue.

Interestingly, we observed cytoplasmic localization of IRX4 in positively stained cells throughout embryogenesis, and early postnatal cardiac tissue, which was not shown in previously reported mRNA detection assays. Results of this study show that Irx4 is maintained in the cytoplasm throughout embryogenesis, and translocates to the nucleus of ventricular CMs on the fifth day of postnatal maturation. We have identified the chromosome region maintenance 1 (CRM1; also known as Exportin 1) pathway as the conduit of IRX4 translocation from the nucleus to the cytoplasm (Fukuda et al., 1997).

Results

IRX4 is co-expressed with markers of the first- or second heart field in the cardiac crescent

Prior to the formation of the cardiac crescent (E7), cardiovascular stem cells have been identified in the lateral plate mesoderm (LPM), adjacent to the primitive streak (David et al., 2011). To determine if IRX4 localized to the LPM, E7.25 wholemount embryos were labeled with an antibody to IRX4 and optically sectioned using confocal microscopy. Compared to Brachyury (T) (Fig. 1A, B), IRX4 was not detected in cells of the cardiac mesoderm, which are a subset of $Brachyury^+$ cells (David et al., 2011) (Fig. 1C,D). Notably, NKX2.5, a regulator of *Irx4* expression, was also not detected at E7.25 in the LPM (Bruneau et al., 2000) (Fig. 1E). However, Nkx2.5, which identifies cardiac progenitors, marked cells of the newly formed cardiac crescent at E7.75 (Wu et al., 2006). Although Irx4 transcripts have been detected in progenitors of the cardiac crescent, our co-immunofluorescence assays, using E7.75 embryos, show that IRX4 was not present in the cardiac progenitors, while $Nkx2.5^+$ cells were detected (Bruneau et al., 2000) (Fig. 1F-H). This result indicates that Irx4 translation either did not occur during the nascent stages of cardiac crescent formation, or the protein had not yet accumulated sufficiently to be detectable by our immunostaining methodology.

We first detected IRX4 at E8.5, after the cardiac crescent has thickened, prior to the formation of the linear heart tube (Fig. 2B, F; see Experimental Procedures for staging). This later cardiac crescent stage (E8.5) is devoid of myocytes, and the developing heart is not yet contracting (Christoffels et al., 2000a).

In situ hybridization data have shown that Irx4 is expressed in the cardiac crescent and later in both ventricular chambers (Christoffels et al., 2000a). The second heart field (SHF) signficantly contributes to the right ventricle, but not the left, while the first heart field (FHF) contributes primarily to the left ventricle (Sun et al., 2007; Verzi et al., 2005; Abu-Issa et al., 2004). Cells positively stained with the Irx4 antibody were detected in the majority of the cells of the crescent, and a subset of this population were positive for TBX5 (Supplemental Movies 1,2), a marker of the FHF. The $IRX4^+/TBX5^+$ population was

observed in the anterior and lateral regions of the cardiac crescent (Fig. 2B-D). IRX4$^-$/TBX5$^+$ cells were found in small regions of posterior tips, and the anterior region of the crescent (arrowheads in figure 2D). IRX4$^+$/TBX5$^-$ cells were abundant in medial and posterior regions of the cardiac crescent (arrows in figure 2D).

Like Tbx5, Islet1 also labels a subset of Irx4$^+$ cells in the cardiac crescent at E8.5. ISLET1$^+$/IRX4$^+$ cells were prominent in the posterior, and dorsal, region of the crescent, while IRX4$^+$/ISLET1$^-$ (arrow in figure 2H) cells were prominent in the anterior of the cardiac crescent (Fig. 2F-H; Supplemental Movies 3,4). A subset of IRX4$^-$/ISLET1$^+$ cells were detected in the posterior branch of the cardiac crescent (arrowhead in figure 2H).

Interestingly, at this stage of cardiogenesis we observed IRX4 in the cytoplasm of cells comprising the cardiac crescent. This subcellular localization differed from the nuclear-restricted expression of TBX5 & ISLET1 (Fig. 2D', H'). Elucidation of IRX4$^+$ cells in the cardiac crescent is an important finding for the continued efforts to resolve the cellular hierarchy responsible for ventricular myocardium differentiation.

IRX4$^+$ cells were restricted to the ventricular region of the linear heart tube at the onset of chamber myocardium development

Following fusion of the cardiac crescent at the mid-line the linear heart tube is formed. At this stage (E8.5-9; see Experimental Procedures for staging) of cardiogenesis regionalization of the developing heart becomes obvious. The anterior portion of the crescent primarily contributes to the ventricular segment, while the posterior tips of the cardiac crescent give rise to the inflow tract. We found that cells positive for IRX4 were restricted to the ventricular segment of the linear heart tube, but were not expressed at the arterial or venous poles of the heart tube (Fig. 3A, B). Co-immunofluorescence experiments show that IRX4 co-localized with NKX2.5 in cells of the ventricular segment (Fig. 3B-D; Supplemental Movies 5, 6). Unlike cells positive for NKX2.5 alone, cells expressing IRX4 protein do not contribute to the venous pole of the heart tube, further supporting the specificity of Irx4 as a genetic marker of the developing ventricular chambers (Fig. 3C-D).

As observed in cells of the cardiac crescent, IRX4 was found in the cytoplasm, while NKX2.5 was restricted to the nuclei of cells of the linear heart tube (Figure 3D').

IRX4$^+$ ventricular myocytes primarily contribute to the compact zone of the developing ventricular myocardium following heart tube looping

While chamber myocardium differentiation commences in the linear heart tube, the heart chambers are not yet formed or positioned properly at that stage of cardiogenesis. Looping of the heart tube (E9-E10) results in positioning of the inflow tract, the precursors of the atria, anterior to the common ventricle. The developing atrial chambers are separated by the outflow tract, which will give rise to the aorta and pulmonary trunk. By E10.5, the chambers are more distinguishable and within the ventricular myocardium there is an emerging distinction between trabeculae, and the compact zone. Anti-IRX4 staining was predominantly observed in the compact zone of the ventricular myocardium at E10.5 (Fig. 4A, B). Cardiac troponin T (cTnT), one of the first contractile proteins expressed specifically in cardiomyocytes, marked myocytes of the compact zone and trabeculae (Fig.

4C,G,K). As the myocardium thickened at later stages of embryogenesis, due to proliferation of ventricular myocytes, IRX4$^+$ cells heavily populated the developing compact zone, with diminished expression in the trabecular region (Fig. 4F,J). This trend, of IRX4$^+$ myocytes contributing significantly to the compact zone of the myocardium and less to the trabeculae, persisted following birth. Cytoplasmic localization of IRX4 in cTnT$^+$ myocytes was maintained from E10.5-14.5 (4D', H', L'). This intracellular localization of IRX4 was maintained throughout embryogenesis (data for later embryonic time points are not shown).

IRX4 exhibits dynamic subcellular localization as the neonatal heart matures

Irx4 transcripts have been detected in neonatal and adult cardiac tissue, maintaining a ventricle-restricted expression pattern as the heart matures following birth. Using immunofluorescence analysis of paraffin-embedded heart sections, we observed IRX4$^+$ cells exclusively in the ventricular myocardium, consistent with our observations of immunostained embryonic sections, described above. Subcellular analysis revealed that IRX4 is was restricted in the cytoplasm throughout embryogenesis and this intracellular localization persisted in postnatal day 2 & 4 hearts (Fig. 5A, B, E, F). In addition to visual confirmation of the intracellular localization of IRX4, we measured the intensity of the fluorescent signal using FIJI (FIJI is just Image J) imaging analysis software. Results of this analysis showed that Irx4 was not detected in the nuclei of myocytes up to postnatal day 4 (Fig. 5U). Irx4 translocates to the nucleus between postnatal days 5-7 and was exclusively detected in the nuclei of cTnT$^+$ myocytes by postnatal day 8 (Fig. 5F, J, N, U). Interestingly, the translocation of IRX4 from the cytoplasm to the nucleus occurred as cardiomyocytes were showing signs of maturation, such as binucleation. The presence of multiple nuclei is indicative of myocyte maturity and a lack of proliferative capacity. Cardiomyocytes at this stage often undergo a final round of DNA synthesis, resulting in mitosis but not cytokinesis (Liu et al., 2010; Bersell et al., 2009). IRX4 was not detected in the cytoplasm of ventricular myocytes from postnatal day 8 onward (Fig. 5M-T)

To further understand the kinetics of the nuclear translocation of Irx4, we prepared primary ventricular myocyte cultures by dissecting and enzymatically digesting the ventricles of postnatal days 2, 4, and 6 hearts. After overnight incubation to allow cell attachment, the cells were considered postnatal days 3, 5, and 7. The cultures were co-stained for IRX4 and cTnT. IRX4 is observed in a diffuse pattern in the cytoplasm of postnatal day 3 myocytes (Fig. 6A-D). Interestingly, the immunofluorescent signal was considerably more concentrated around the nucleus, with diffuse expression in other parts of the cytoplasm. IRX4 was detected in both the nucleus and cytoplasm of postnatal day 5 myocytes. The signal began to accumulate in the nucleus, with diffuse expression in the cytoplasm (Fig. 6E, F, M). Nuclear fluorescence intensity was significantly higher in postnatal day 5 myocytes when compared to postnatal day 3 cells. By postnatal day 7, IRX4 was exclusively detected in the nuclei (Fig. 6I-L, M). These immunostaining results with the primary myocyte cultures not only defined the time course of the change of IRX4 subcellular localization, but shows that migration to the nucleus begins at day 5 of postnatal maturation.

The CRM1 pathway is responsible for IRX4 subcellular translocation

Our results show that throughout embryogenesis Irx4 protein was detected exclusively in the cytoplasm of immature ventricular cardiomyocytes, and was not found in the nucleus until postnatal day 5. This lengthy cytosolic restriction is unusual, as other transcription factors, such as Mef2c, exhibit transient translocation to the cytoplasm during cardiomyocyte differentiation (Munoz et al., 2009). To determine the mode of translocation, we first performed peptide sequence analysis and identified a putative nuclear export signal (NES) (LSDLEDFDP). The motif is primarily comprised of hydrophobic residues, and similar to that found in T-box transcription factors (Kulisz et al., 2008). T-box factors containing this NES are shuttled from the nucleus to the cytoplasm via the chromosome region maintenance 1 (CRM1) pathway. To determine whether Irx4 employs this mode of intracellular translocation, we disrupted the CRM1 pathway in primary E12.5 myocytes, when Irx4 expression is cytoplasmic, using the antibiotic Leptomycin B (Kudo et al., 1998; Sun et al., 2013). Even when maintained in vitro, these ventricular myocytes continued to exhibit cytoplasmic IRX4 (Fig. 7B, J). Following overnight incubation with Leptomycin B, IRX4 was detected in the nucleus, suggesting that the antibiotic prevented translocation of IRX4 to the cytoplasm, indicating that the CRM1 pathway is involved in the movement of IRX4 from the nucleus to the cytoplasm (Fig. 7F). Localization of IRX4 within the cells was reflected by fluorescence intensity, which correlates with pixel measurements. We observed a significant increase of fluorescence intensity in the nuclei of myocytes treated with Leptomycin B, confirming that IRX4 was held in the nucleus when the CRM1 pathway was blocked (Fig. 7M)

Discussion

In this study, we elucidated the spatial and temporal localization of Irx4 protein during murine embryogenesis. To the best of our knowledge, this is the first study to localize IRX4, as all previous studies focused on RNA expression of this homeobox transcription factor (Bruneau et al., 2000; Christoffels et al., 2000b). Our whole-mount embryo immunofluorescence assay results show that $IRX4^{+}$ cells contribute to the cardiac crescent. Given the ventricle-specific expression of Irx4 at later stages of cardiogenesis, the presence of $IRX4^{+}$ cells in the crescent suggests that ventricular myocardium specification occurs prior to formation of the linear heart tube. To address this hypothesis, lineage tracing experiments must be employed.

Lineage tracing experiments have shown that cells of the cardiac crescent represent cardiac progenitor populations that contribute to heart formation (Moretti et al., 2006; Ma et al., 2008). Using in situ hybridization, several groups have identified Irx4 transcripts in a spatial pattern which suggests that the transcription factor labels cardiac progenitors (Bruneau et al., 2000; Christoffels et al., 2000a&b). Results of the present study further our understanding of the $Irx4^{+}$ cells that have previously been identified using transcript detection assays. IRX4 was found in cells of the cardiac crescent, along with TBX5 or ISLET1, which have been established as markers of the first and second heart fields, respectively (Herrmann et al., 2011; Engleka et al., 2012). The subpopulations of $IRX4^{+}/TBX5^{+}$ or $IRX4^{+}/ISLET1^{+}$ cells, identified in this study using an antibody staining approach, suggest that the $IRX4^{+}$ cells of

the crescent potentially encompass two distinct progenitor pools. Because Irx4 is expressed in both ventricular chambers, while Tbx5 or Islet1 expression is restricted to the left and right ventricle, respectively, it is reasonable to hypothesize that Irx4 labels two distinct ventricular progenitors in the cardiac crescent (Herrmann et al., 2011; Engleka et al., 2012; Domian et al., 2009). The identification of putative left- and right ventricular progenitors is important for understanding the cellular dynamics responsible for the allocation of cells to distinct ventricular chambers. Given the identification of cardiac crescent cells positive for IRX4, and the ventricle-specific localization of $IRX4^+$ cells following chamber formation, this transcription factor appears to be an ideal marker for isolating ventricular progenitors that can contribute to cell therapeutic approaches to ameliorate insult to the ventricular myocardium.

Irx4 is one of the first markers to label immature myocytes of the nascent ventricular myocardium in the linear heart tube at E9. This heart chamber specificity is maintained throughout murine embryogenesis (Christoffels et al., 2000a). We show that IRX4 was restricted to the ventricular segment of the linear heart tube, which differs from transcript detection data published by Christoffels and colleagues detecting Irx4 transcripts in the posterior region of the outflow tract, and anterior portion of the inflow tract (Christoffels et al., 2000a). The discrepancy in these observations could be due to migration of $Irx4^+$ cells from adjacent regions of the heart to the medially located ventricular segment. The translation pattern in this study follows the spatial and temporal RNA expression pattern shown by Bruneau and colleagues, which highlights a clear boundary of Irx4 expression between the ventricular region of the heart tube (linear and looping) and venous or arterial poles. In this same study, an obvious demarcation of Irx4 expression between the ventricular and atrial (inflow tract) segments of the linear heart tube was displayed (Bruneau et al., 2000). Within the developing myocardium, following looping of the linear heart tube, $IRX4^+$ cells were predominantly observed in the expanding compact zone during the later stages of heart development in the mouse embryo. Thickening of the compact zone during embryogenesis is a result of cell division, and the prescence of IRX4 in the dividing myocytes indicates that the transcription factor is expressed in immature, cycling ventricular myoctyes (Sedmera and Thompson et al., 2011).

Interestingly, we found that in embryonic and neonatal cardiac tissue IRX4 localized to the cytoplasm. Cytoplasmic localization of IRX4 in immature myocytes is likely due to the presence of a leucine-rich nuclear export sequence, which is recognized by CRM1 (Fukuda et al., 1997). In postnatal day 5-6 hearts, IRX4 is shuttled into the nucleus of ventricular myocytes due to the presence of a nuclear localization signal, and this translocation correlates with the loss of myocyte proliferative capacity, signified by an increase of bi-nucleated myocytes in the ventricular myocardium (Li et al., 1996).

Recent reports show that myocyte turnover is significantly diminished after postnatal day 7 (Porrello et al., 2011). The miR-15 family appears to drive the downregulation of proliferation markers in the maturing cardiomyocytes, along with the expression of Meis1(Porrello et al., 2013; Mahmoud et al., 2013). Genome profiling of neonatal heart tissue, indicates that proliferation markers (Ki67, PCNA) are significantly downregulated in postnatal day 7 hearts compared to newborn (day 0) hearts (Chen et al., 2004). After

myocytes cease to proliferate, the primary source of heart growth is hypertrophy. Conversely, markers of mature myocytes such as Junctophilin-2, which is necessary for transverse tubule maturation, are upregulated as expression of proliferation markers diminish (Reynolds et al., 2013). Nuclear translocation of IRX4 appears to coincide with a significant change in the gene expression profile of myocytes. The relationship between IRX4 subcellular localization and myocyte proliferation warrants further investigation, with a specific focus on the regulatory function of IRX4 in the cytoplasm and nucleus of cardiomyocytes, and the signal(s) responsible for IRX4 cytoplasmic tethering and nuclear translocation.

Dynamic subcellular localization of IRX4 suggests that this transcription factor plays multiple roles within myocytes, and these roles change as the cells mature. When *Irx4* expression is ablated in the mouse, cardiogenesis occurs normally, with functional ventricular myocytes contributing to a healthy myocardium (Bruneau et al., 2000). Effects of this *Irx4* mutation manifest in adult myocytes, which according to our results, express IRX4 in the nucleus. The lack of a mutant phenotype during embryogenesis implies that IRX4 doesn't function as a gene regulator during embryogenesis.

Elucidation of novel ventricle-specific cell types that facilitate ventricular myocardium differentiation have considerable biological and clinical implications. In this study we have shown that $IRX4^+$ cells in the cardiac crescent co-express markers of the first- or second heart fields at E8.5. Given that $IRX4^+$ cells are restricted to the ventricular segment at E9, our findings suggest that ventricular myocardium specification occurs in the cardiac crescent, preceding linear heart tube formation. We propose that tracking $IRX4^+$ cells during cardiogenesis will contribute significantly to resolving the cell dynamics responsible for the development of the myocardial layer of both ventricular chambers.

Experimental Procedures

Embryo preparations

For whole-mount immunofluorescence (IF) staining, we used BALBc mice without genetic modification. Mice were maintained on a 12-hour light/dark cycle (lights off: 18.00/lights on: 6.00). Timed matings were carried out to assure accuracy of embryo staging (Champlin et al., 1973). Noon, the day following pairing, was considered day 0.5.

In this report, we have integrated the widely accepted morphological staging system of Downs and Davies (1993) with embryonic days post-coitum in the BALB/c mouse strain according to the light/dark cycle used here, the timing of plug detection, and with the morphological stage of the heart as follows:

- **i.** onset of cardiogenesis (E6.5); this corresponds to the onset of gastrulation and mesoderm formation
- **ii.** formation of the cardiac crescent (E7.5-8.5); we found evidence for the early crescent at the early headfold stage (E7.75), and the late crescent at 4-6-somite pairs (E8-8.5);
- **iii.** formation of the linear heart tube (E8.5-9.0),

iv. heart looping (E9.0-10.0), and

v. septation of the ventricular chamber (E10.5-11.5)

Correlating these three parameters provides an unprecedented degree of accuracy in staging the heart than is presently available in the literature. We chose this system because the variation in staging of embryos is affected by the time of mating in the 12 hour dark cycle and the 12+ hour variability than can occur within any litter. Also, it is possible that differences between our staging and that commonly described elsewhere may be due to strain variability.

For E7-7.25 samples, the chorion was maintained. Reichert's membrane was reflected, and the anterior portion of the yolk sac was breached in embryos E8 or older to allow for antibody penetration. Following embryo dissection, the samples were rinsed in 1× PBS and fixed with 4% paraformaldehyde (Sigma), prepared in 1× PBS, at 4°C, for 45 minutes with gentle agitation. Embryos were dehydrated with a gradient of increasing concentrations (25, 50, 75, & 100%) of methanol (Fisher Scientific) prepared in deionized water for storage at -20°C. Colony maintenance, experimental procedures and euthanasia of mice were approved by the Institutional Animal Care and Use Committee of the University of Wisconsin School of Medicine & Public Health.

Whole-mount embryo embedding and antibody staining

Embryos were rehydrated with a decreasing gradient (100, 75, 50, & 25%) of methanol, and rinsed twice in 1× PBS. Embryos were incubated twice in blocking solution (1× PBS, 0.1% Triton x-100, and 10% serum) with gentle agitation for 1 hour. Embryos were incubated with the primary antibody solution (primary antibody diluted in blocking solution) overnight at 4°C. Secondary antibodies (Invitrogen) were incubated with embryos overnight at 4°C, following five, 1 hour rinses in blocking solution. Embryos were rinsed with blocking solution and samples were oriented and embedded in 2% agarose (Promega) on coverslips. Coverslips, with embedded embryos attached, were mounted onto concave glass slides (Varsity Glass). For each whole-mount IF assay we used 2 embryos/immunostain. Whole-mount IF experiments for each embryonic stage were repeated 4 times. The following antibodies were used in this study: Goat anti-Irx4 N-16 IgG (SCBT-22582 200μg/ml [1:100]), Mouse anti-Irx4 IgM (Abgent 600μg/ml [1:500]), Goat anti-Brachyury (SCBT-17743 200μg/ml [1:500]), Goat anti-Nkx 2.5 IgG (R&D Biosystems-AF2444 100μg/ml [1:250]), Rabbit anti-Tbx5 IgG (Abcam-ab18531 400μg/ml [1:100]), Rabbit anti-Islet1 IgG (SCBT-30200 200μg/ml [1:100]), Mouse anti-cardiac troponin T IgG (Neomarkers-MS295P1 200μg/ml [1:250]).

Embryonic, post-natal and adult heart preparations

Hearts were dissected at post-natal days 2, 4, 6, 8, & 10. Adult heart samples were dissected from 1 and 2 month old female mice. Following dissection, hearts were rinsed briefly in 1× PBS. Hearts were incubated in 4% paraformaldehyde overnight, at 4°C with gentle agitation. Fixed hearts were dehydrated and embedded in paraffin under vacuum (25 hg) at 62°C in preparation for sectioning. All heart sections were 5μm thick. E10.5-14.5 embryos were rinsed in 1× PBS and incubated with 4% paraformaldehyde at 4°C, for 2 hours. Embryos

were embedded in paraffin and sectioned to a thickness of 10μm. Sections were boiled in sodium citrate, 0.05% Tween-20 solution for 30 minutes to unmask the antigens. The sections were then rinsed with 1× PBS (3 times, 5 minutes each), followed by an eight minute rinse in 1% saponin (Sigma) solution. Sections were then rinsed in 1× PBS plus 5% Triton X-100 and blocked in a solution containing 5% animal serum and 0.1% Triton X-100 diluted in 1× PBS. Sections were placed at 37°C for 45 minutes to block the tissue. Primary antibodies were incubated on sections overnight at room temperature. Following three washes in 1× PBS plus Triton X-100, the sections were incubated in secondary antibody solution (fluorescent secondary antibodies were diluted 1:200 in blocking solution) for 2 hours at room temperature. All secondary antibodies are supplied at a stock concentration of 2mg/ml (Invitrogen). Immunofluorescence experiments for each embryonic and postnatal time point were repeated 3 times.

Microscopy

The Leica TCS SP5 confocal microscopy system was employed to observe results of whole-mount embryo immunostained preparations. Confocal microscopy was performed using the 10× objective (numerical aperture of 0.3, resolution max in XY= 4768, resolution in Z= 651, and working distance= 11000μm), or 40× objective (numerical aperture of 1.3, resolution max in XY= 150, resolution in Z= 299, and working distance= 220μm). We maintained a setting of 27% power to the Argon laser for all confocal microscopy sessions. To ensure that the images were comparable, we kept laser power at 13% for 488 and 568 wavelengths, while the UV light was fixed at setting 7. Epifluorescence samples were observed and imaged using the Zeiss Axiovert 200 microscope, with a Nikon CCD camera connected.

Primary myocyte preparations & Leptomycin B treatments

Mouse ventricles were dissected from E12.5 embryos and atria discarded. After being rinsed in PBS, the samples were incubated at 37°C in digestion solution (2.5% trypsin, 1% collagenase, chicken serum, and Hank's Buffer Saline Solution) supplemented with 1μl of DNase I (1unit/μl). Tissue samples were pipetted (gently) several times, then incubated with fresh digestion solution after collection of the supernatant. Samples were pelleted and resuspended in DMEM (Invitrogen)+10%FBS (Gibco). Cells were pre-plated for 15 minutes using uncoated tissue culture dishes to remove fibroblasts from the preparations. Myocytes were plated into wells of a 24-well dish, containing 1% gelatin-coated glass coverslips. Cells were incubated in DMEM+10%FBS overnight, before changing medium the next morning.

Leptomycin B (Sigma) treatments were performed as described by Kulisz, A et al (2008). Leptomycin B (supplied at 1μg/ml in 70% methanol) was added to DMEM+10%FBS medium at a final concentration of 1nM. Observations were made and photographs taken using the Leica TCS SP5 confocal system. The 20x objective used for observations has a numerical aperture of 0.7, resolution max in XY= 278.9, resolution in Z= 1284, and working distance= 0.59mm. Experiments using Leptomycin B treatments were repeated with 3 independent primary embryonic myocyte preparations.

Image & statistical analysis

Pixel intensity was determined for immunofluorescence samples using FIJI image analysis software. Regions of interest (ROI) were outlined around random nuclei using images that show DNA labeled with hoechst dye. By labeling nuclei in the nuclear counterstain image, the ROI selections were unbiased. At least 20 ROIs were selected from a single image, and 3 images were used for each sample. Each image was from an independent experiment. Microscope settings were maintained for each experiment so the results were comparable. Intensity measurements were compiled and analyzed for a one-way ANOVA in Prism 6 program. Significance= $p < 0.05$

Supplementary Material

Refer to Web version on PubMed Central for supplementary material.

Acknowledgments

We thank Dr. Aseem Ansari for the Nkx2.5 polyclonal antibody. We also thank Maria Mikedis in the Downs Lab for scientific support, and Dr. Jayne Squirrell for her guidance with the statistical analysis. This study was supported by NIH grant numbers HL1051092 (pre-doctoral NRSA), HL084615 (R01), and American Heart Assoc grant number 0650032Z.

References

Abu-Issa R, Waldo K, Kirby ML. Heart fields: one, two or more? Dev Biol. 2004; 272:281–285. [PubMed: 15282148]

Anderson RH, Webb S, Brown NA, Lamers W, Moorman A. Development of the heart: (2) Septation of the atriums and ventricles. Heart. 2003; 89:949–958. [PubMed: 12860885]

Bao ZZ, Bruneau BG, Seidman JG, Seidman CE, Cepko CL. Regulation of chamber-specific gene expression in the developing heart by Irx4. Science. 1999; 283:1161–1164. [PubMed: 10024241]

Bersell K, Arab S, Haring B, Kuhn B. Neuregulin1/ErbB4 signaling induces cardiomyocyte proliferation and repair of heart injury. Cell. 2009; 138:257–270. [PubMed: 19632177]

Bruneau BG, Bao ZZ, Tanaka M, Schott JJ, Izumo S, Cepko CL, Seidman JG, Seidman CE. Cardiac expression of the ventricle-specific homeobox gene Irx4 is modulated by Nkx2-5 and dHand. Dev Biol. 2000; 217:266–277. [PubMed: 10625552]

Bruneau BG, Bao ZZ, Fatkin D, Xavier-Neto J, Georgakopoulos D, Maguire CT, Berul CI, Kass DA, Kuroski-de Bold ML, de Bold AJ, Conner DA, Rosenthal N, Cepko CL, Seidman CE, Seidman JG. Cardiomyopathy in Irx4-deficient mice is preceded by abnormal ventricular gene expression. Mol Cell Biol. 2001; 21:1730–1736. [PubMed: 11238910]

Bruneau BG, Logan M, Davis N, Levi T, Tabin CJ, Seidman JG, Seidman CE. Chamber-specific cardiac expression of Tbx5 and heart defects in Holt-Oram syndrome. Dev Biol. 1999; 211:100–108. [PubMed: 10373308]

Champlin AK, Dorr DL, Gates AH. Determining the stage of the estrous cycle in the mouse by the appearance of the vagina. Biol Reprod. 1973; 8:491–494. [PubMed: 4736343]

Chen HW, Yu SL, Chen WJ, Yang PC, Chien CT, Chou HY, Li HN, Peck K, Huang CH, Lin FY, Chen JJ, Lee YT. Dynamic changes of gene expression profiles during postnatal development of the heart in mice. Heart. 2004; 90:927–934. [PubMed: 15253972]

Christoffels VM, Habets PE, Franco D, Campione M, de Jong F, Lamers WH, Bao ZZ, Palmer S, Biben C, Harvey RP, Moorman AF. Chamber formation and morphogenesis in the developing mammalian heart. Dev Biol. 2000a; 223:266–278. [PubMed: 10882515]

Christoffels VM, Keijser AG, Houweling AC, Clout DE, Moorman AF. Patterning the embryonic heart: identification of five mouse Iroquois homeobox genes in the developing heart. Dev Biol. 2000b; 224:263–274. [PubMed: 10926765]

David R, Jarsch VB, Schwarz F, Nathan P, Gegg M, Lickert H, Franz WM. Induction of MesP1 by Brachyury(T) generates the common multipotent cardiovascular stem cell. Cardiovasc Res. 2011; 92:115–122. [PubMed: 21632880]

Domian IJ, Chiravuri M, van der Meer P, Feinberg AW, Shi X, Shao Y, Wu SM, Parker KK, Chien KR. Generation of functional ventricular heart muscle from mouse ventricular progenitor cells. Science. 2009; 326:426–429. [PubMed: 19833966]

Downs KM, Davies T. Staging of gastrulating mouse embryos by morphological landmarks in the dissecting microscope. Development. 1993; 118:1255–1266. [PubMed: 8269852]

Dyer LA, Kirby ML. The role of secondary heart field in cardiac development. Dev Biol. 2009; 336:137–144. [PubMed: 19835857]

Engleka KA, Manderfield LJ, Brust RD, Li L, Cohen A, Dymecki SM, Epstein JA. Islet1 derivatives in the heart are of both neural crest and second heart field origin. Circ Res. 2012; 110:922–926. [PubMed: 22394517]

Evans SM, Yelon D, Conlon FL, Kirby ML. Myocardial lineage development. Circ Res. 2010; 107:1428–1444. [PubMed: 21148449]

Fishman GI. Understanding conduction system development: a hop, skip and jump away? Circ Res. 2005; 96:809–811. [PubMed: 15860760]

Francou A, Saint-Michel E, Mesbah K, Theveniau-Ruissy M, Rana MS, Christoffels VM, Kelly RG. Second heart field cardiac progenitor cells in the early mouse embryo. Biochim Biophys Acta. 2013; 1833:795–798. [PubMed: 23051926]

Fukuda M, Asano S, Nakamura T, Adachi M, Yoshida M, Yanagida M, Nishida E. CRM1 is responsible for intracellular transport mediated by the nuclear export signal. Nature. 1997; 390:308–311. [PubMed: 9384386]

Herrmann F, Bundschu K, Kuhl SJ, Kuhl M. Tbx5 overexpression favors a first heart field lineage in murine embryonic stem cells and in Xenopus laevis embryos. Dev Dyn. 2011; 240:2634–2645. [PubMed: 22072574]

Kim KH, Rosen A, Bruneau BG, Hui CC, Backx PH. Iroquois homeodomain transcription factors in heart development and function. Circ Res. 2013; 110:1513–1524. [PubMed: 22628575]

Kitajima S, Takagi A, Inoue T, Saga Y. MesP1 and MesP2 are essential for the development of cardiac mesoderm. Development. 2000; 127:3215–3226. [PubMed: 10887078]

Kubalak SW, Miller-Hance WC, O'Brien TX, Dyson E, Chien KR. Chamber specification of atrial myosin light chain-2 expression precedes septation during murine cardiogenesis. J Biol Chem. 1994; 269:16961–16970. [PubMed: 8207020]

Kudo N, Wolff B, Sekimoto T, Schreiner EP, Yoneda Y, Yanagida M, Horinouchi S, Yoshida M. Leptomycin B inhibition of signal-mediated nuclear export by direct binding to CRM1. Exp Cell Res. 1998; 242:540–547. [PubMed: 9683540]

Kulisz A, Simon HG. An evolutionarily conserved nuclear export signal facilitates cytoplasmic localization of the Tbx5 transcription factor. Mol Cell Biol. 2008; 28:1553–1564. [PubMed: 18160705]

Li F, Wang X, Capasso JM, Gerdes AM. Rapid transition of cardiac myocytes from hyperplasia to hypertrophy during postnatal development. J Mol Cell Cardiol. 1996; 28:1737–1746. [PubMed: 8877783]

Liang X, Wang G, Lin L, Lowe J, Zhang Q, Bu L, Chen YH, Chen J, Sun Y, Evans SM. HCN4 Dynamically Marks the First Heart Field and Conduction System Precursors. Circ Res. 2013

Liu Z, Yue S, Chen X, Kubin T, Braun T. Regulation of cardiomyocyte polyploidy and multinucleation by CyclinG1. Circ Res. 2010; 106:1498–1506. [PubMed: 20360255]

Ma Q, Zhou B, Pu WT. Reassessment of Isl1 and Nkx2-5 cardiac fate maps using a Gata4-based reporter of Cre activity. Dev Biol. 2008; 323:98–104. [PubMed: 18775691]

Mahmoud AI, Kocabas F, Muralidhar SA, Kimura W, Koura AS, Thet S, Porrello ER, Sadek HA. Meis1 regulates postnatal cardiomyocyte cell cycle arrest. Nature. 2013; 497:249–253. [PubMed: 23594737]

Moorman A, Webb S, Brown NA, Lamers W, Anderson RH. Development of the heart: (1) formation of the cardiac chambers and arterial trunks. Heart. 2003; 89:806–814. [PubMed: 12807866]

Moretti A, Caron L, Nakano A, Lam JT, Bernshausen A, Chen Y, Qyang Y, Bu L, Sasaki M, Martin-Puig S, Sun Y, Evans SM, Laugwitz KL, Chien KR. Multipotent embryonic isl1+ progenitor cells lead to cardiac, smooth muscle, and endothelial cell diversification. Cell. 2006; 127:1151–1165. [PubMed: 17123592]

Munoz JP, Collao A, Chiong M, Maldonado C, Adasme T, Carrasco L, Ocaranza P, Bravo R, Gonzalez L, Diaz-Araya G, Hidalgo C, Lavandero S. The transcription factor MEF2C mediates cardiomyocyte hypertrophy induced by IGF-1 signaling. Biochem Biophys Res Commun. 2009; 388:155–160. [PubMed: 19654000]

Porrello ER, Mahmoud AI, Simpson E, Hill JA, Richardson JA, Olson EN, Sadek HA. Transient regenerative potential of the neonatal mouse heart. Science. 2011; 331:1078–1080. [PubMed: 21350179]

Porrello ER, Johnson BA, Aurora AB, Simpson E, Nam YJ, Matkovich SJ, Dorn GW 2nd, van Rooij E, Olson EN. MiR-15 family regulates postnatal mitotic arrest of cardiomyocytes. Circ Res. 2013; 109:670–679. [PubMed: 21778430]

Reynolds JO, Chiang DY, Wang W, Beavers DL, Dixit SS, Skapura DG, Landstrom AP, Song LS, Ackerman MJ, Wehrens XH. Junctophilin-2 is necessary for T-tubule maturation during mouse heart development. Cardiovasc Res. 2013

Saga Y, Kitajima S, Miyagawa-Tomita S. Mesp1 expression is the earliest sign of cardiovascular development. Trends Cardiovasc Med. 2000; 10:345–352. [PubMed: 11369261]

Sedmera D, Thompson RP. Myocyte proliferation in the developing heart. Dev Dyn. 2011; 240:1322–1334. [PubMed: 21538685]

Solloway MJ, Harvey RP. Molecular pathways in myocardial development: a stem cell perspective. Cardiovasc Res. 2003; 58:264–277. [PubMed: 12757862]

Sun Q, Carrasco YP, Hu Y, Guo X, Mirzaei H, Macmillan J, Chook YM. Nuclear export inhibition through covalent conjugation and hydrolysis of Leptomycin B by CRM1. Proc Natl Acad Sci U S A. 2013; 110:1303–1308. [PubMed: 23297231]

Sun Y, Liang X, Najafi N, Cass M, Lin L, Cai CL, Chen J, Evans SM. Islet 1 is expressed in distinct cardiovascular lineages, including pacemaker and coronary vascular cells. Dev Biol. 2007; 304:286–296. [PubMed: 17258700]

Verzi MP, McCulley DJ, De Val S, Dodou E, Black BL. The right ventricle, outflow tract, and ventricular septum comprise a restricted expression domain within the secondary/anterior heart field. Dev Biol. 2005; 287:134–145. [PubMed: 16188249]

Vincent SD, Buckingham ME. How to make a heart: the origin and regulation of cardiac progenitor cells. Curr Top Dev Biol. 2010; 90:1–41. [PubMed: 20691846]

Wu SM, Fujiwara Y, Cibulsky SM, Clapham DE, Lien CL, Schultheiss TM, Orkin SH. Developmental origin of a bipotential myocardial and smooth muscle cell precursor in the mammalian heart. Cell. 2006; 127:1137–1150. [PubMed: 17123591]

Abbreviations

CRM1	chromosome region maintenance 1
cTnT	cardiac troponin T
FHF	first heart field
FIJI	FIJI is just image J
Irx4	Iroquois related homeobox protein 4
Mef2c	myocyte enhancer factor 2c
Mesp1	mesoderm posterior 1
Myl2	myosin light chain 2V

Nkx2.5	Nk2 homeobox 5
SHF	second heart field
Tbx5	T-box 5

Bullet points

I. Ventricular myocardium specification occurs in the cardiac crescent

II. IRX4+ cells in the cardiac crescent co-express markers of both heart fields

III. IRX4 exhibits dynamic intracellular localization in maturing cardiomyocytes

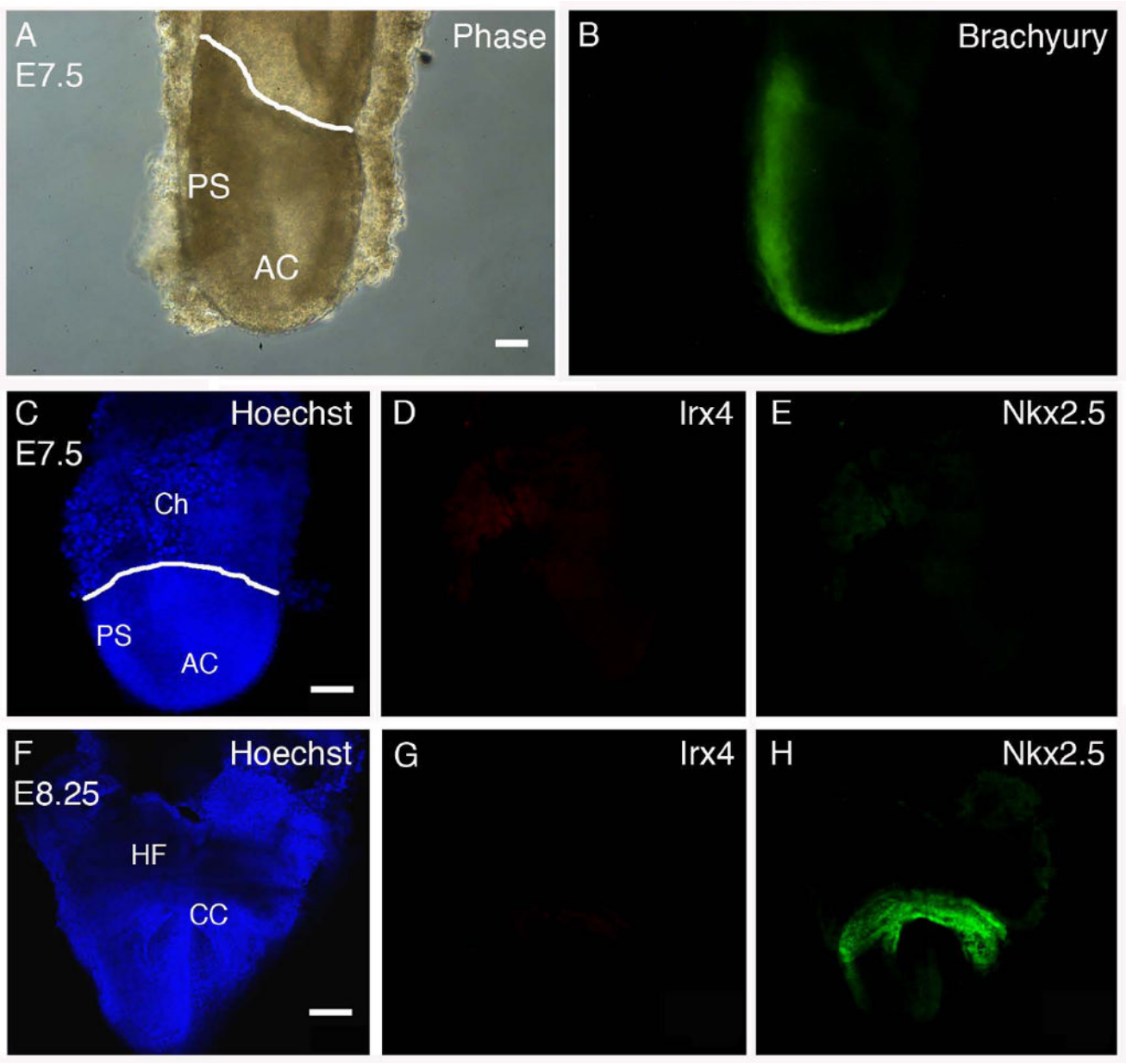

Figure 1. IRX4^{+} cells are absent from the cardiac mesoderm progenitor pool and cardiac progenitor populations of the early cardiac crescent

(A,B) Phase-contrast image (A) of E7.0 (late streak stage, Downs and Davies, 1993) conceptus shown in (B), immunostained for Brachyury. Conceptus was imaged in sagittal orientation. (C-E) Neural plate stage conceptus (E7.25, Downs and Davies, 1993) co-immunostaining with Hoechst (C), anti-IRX4 (D), and anti-NKX2.5 (E). The white line in panels A, C marks the separation between extra-embryonic and embryonic tissue. E7.25 conceptus was imaged in a sagittal orientation. (F-G) Epifluorescence images of an E7.75 (early headfold, Downs and Davies, 1993; early crescent stage) conceptus in frontal view counterstained with Hoechst dye (F), and co-immunostained with IRX4 (G) and NKX2.5 (H) antibodies. Abbreviations: AC, amniotic cavity; CC, cardiac crescent; Ch, chorion; HF, head folds; PS, primitive streak. Scale bar (A, C, F), 100μm.

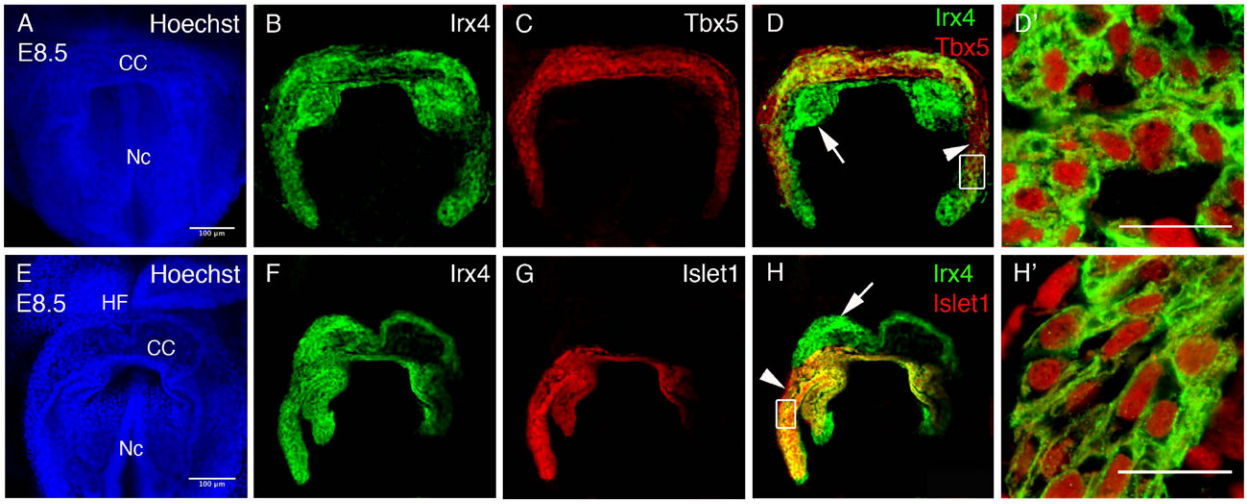

Figure 2. IRX4^{+} cells contribute to the first and second heart fields

E8.5 conceptuses (4-6s, Downs and Davies, 1993; late crescent stage) in frontal view; (A-D and E-H represent two different conceptuses). (A, E) Hoechst, (B, F) IRX4, (C) TBX5, and (G) ISLET1. The Alexa fluor-488 (B, F) and -568 channels (C, G) were merged (D, H, respectively). Abbreviations: HF, head folds; CC, cardiac crescent; Nc, Notochord. Scale bar (A, E), 100μm. Arrows (D, H) point to IRX4^{+}/TBX5^{-} (D) or IRX4^{+}/ISLET1^{-} (H) cells of the cardiac crescent. Arrowheads (D, H) point to IRX4^{-}/TBX5^{+} (D) or IRX4^{-}/ISLET1^{+} (H) cells of the cardiac crescent. Panels D' and H' are magnified images of boxed regions in panels D and H, respectively. Scale bar in panels D' and H', 25μm. Images in each panel are a single focal plane acquired using the confocal microscope.

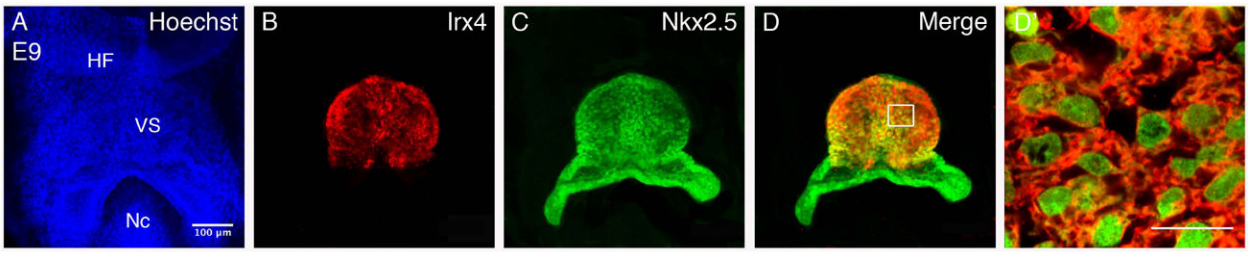

Figure 3. IRX4 labels immature ventricular myocytes at the onset of myocardium differentiation

Confocal microscopy of an E9 conceptus. (A) Hoechst (B) IRX4, and (C) NKX2.5. (D) Alexa fluor 488 and 568 channels were merged to illustrate the relation of $IRX4^{+}$ and $NKX2.5^{+}$ cells in the heart tube. Panel D' is a magnified image of the boxed region in panel D. Images represent a single focal plane. The embryo was oriented in frontal orientation, and images were obtained using confocal microscopy. Images represent a single focal plane. Abbreviations: HF, head folds; VS, ventricular segment; IT, inflow tract; Nc, Notochord. Scale bar for A, 100µm, and scale bar for D', 25µm.

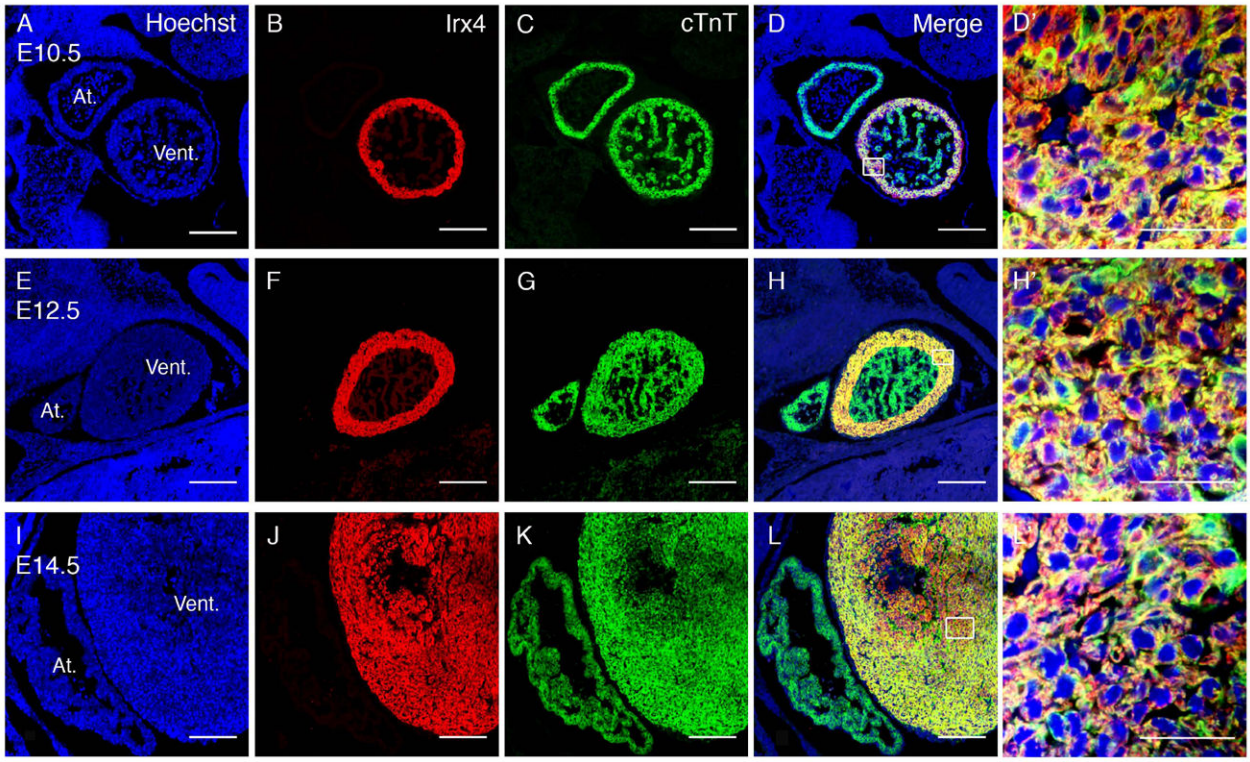

Figure 4. IRX4^{+} myocytes primarily contribute to the compact ventricular myocardium

Confocal microscopy images of embryonic sections in sagittal orientation. (A,E,I) Hoechst stain. (B, F, J) Irx4 stain, (C, G, K) and Cardiac troponin T stain of E10.5, 12.5, 14.5 embryonic sections, respectively. (D, H, L) Alexa fluor 488 and -568 channels were merged to illustrate the relation of IRX4^{+} and cTnT^{+} cells in the developing heart. Panels D', H', and L' are magnified images of the boxed regions in panels D, H, and L, respectively. All sections were embedded in paraffin prior to sectioning. Each panel represents a single focal plane. Abbreviations: At, Atrium; Vent., Ventricle. Scale bar all panels, 50μm. Scale bar for D', H', L', 25μm.

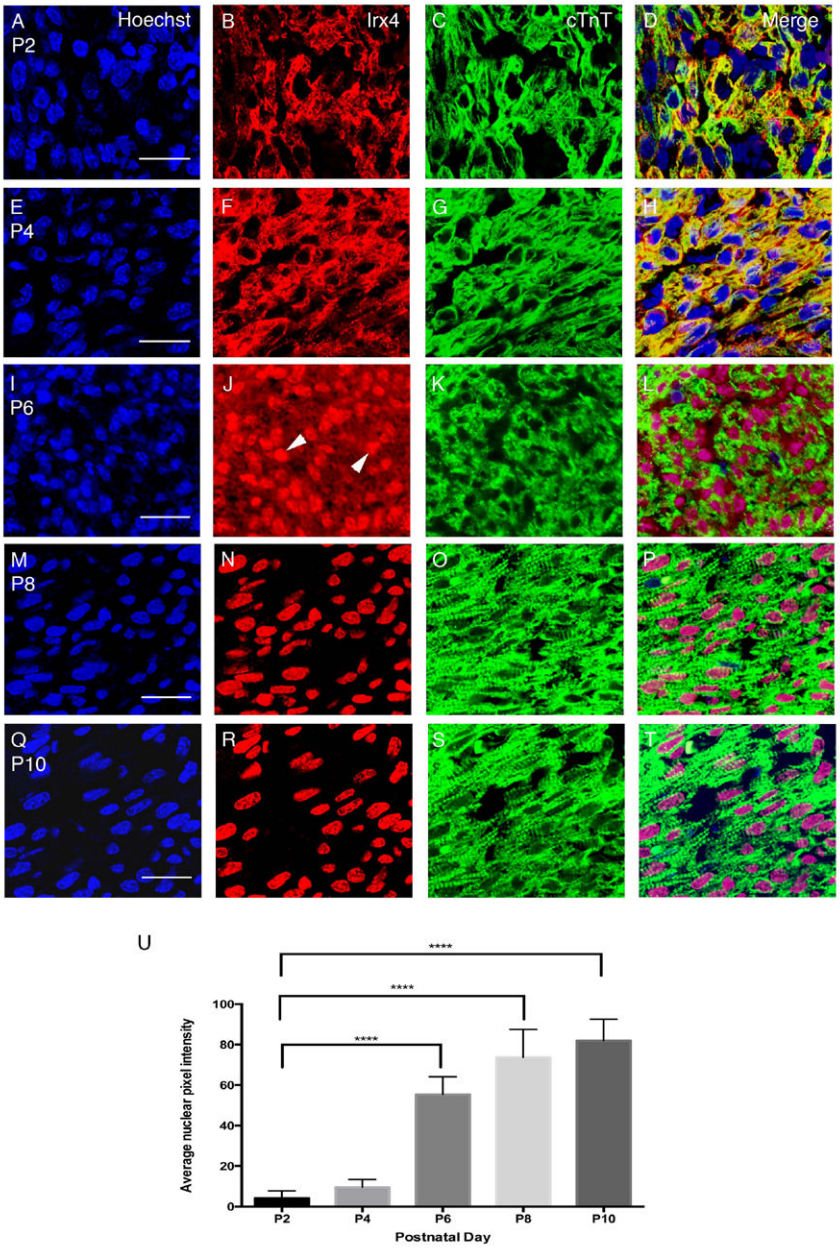

Figure 5. IRX4 exhibits dynamic subcellular localization in neonatal cardiac tissue

Neonatal and early postnatal cardiac tissue was imaged using confocal microscopy. Each panel represents a single focal plane. (A-C) Postnatal day 2 heart sections stained for (A) Hoechst, (B) Irx4, and (C) cardiac troponin T. (E-G) Postnatal day 4 heart sections stained for (E) Hoechst, (F) Irx4, and (G) cardiac troponin T. (I-K) Postnatal day 6 heart sections stained for (I) Hoechst, (J) Irx4, and (K) cardiac troponin T. (M-O) Postnatal day 8 heart sections stained for (M) Hoechst, (N) Irx4, and (O) cardiac troponin T. (Q-S) Postnatal day 10 heart sections stained for (Q) Hoechst, (R) IRX4, and (S) cTnT. (D, H, L, P, I) Alexa fluor 488 and -568 channels were merged to illustrate the relation of IRX4 and cTnT at the subcellular level in ventricular myocytes of the postnatal day 2, 4, 6, 8, and 10 ventricular myocardium, respectively. (U) Graph depicting the mean pixel intensity within the nuclei. Errors represent standard deviation. n=62. ****P < 0.0001. Arrowheads in J highlight nuclei positive for IRX4. Abbreviations: P=postnatal. Scale bars, 25μm.

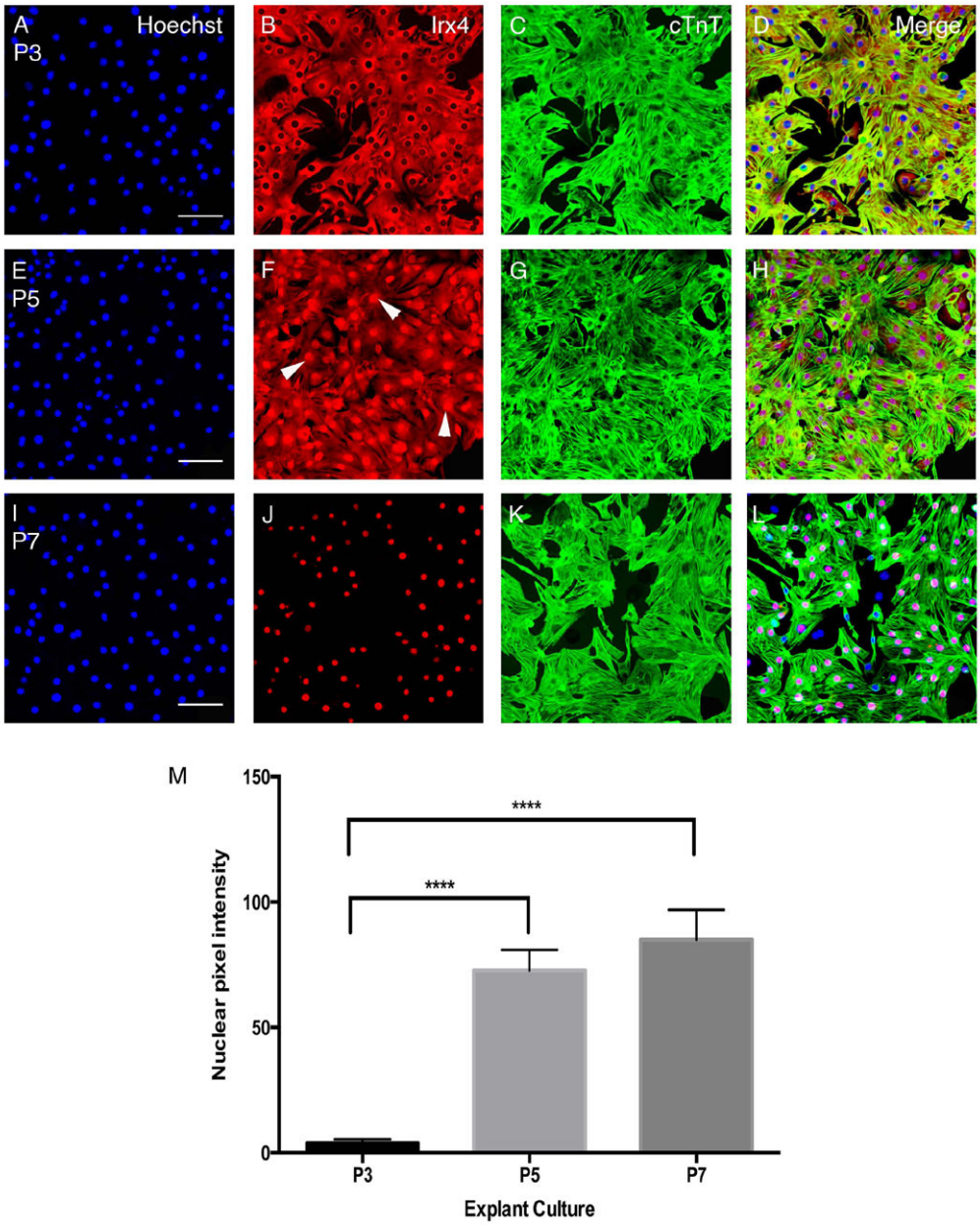

Figure 6. IRX4 exhibits dynamic intracellular localization in cardiac explant cultures

Confocal microscopy of cardiomyocyte explant cultures. Each panel represents a single focal plane. (A, E, I) Hoecsht stain of explant cultures for postnatal day 3, 5, and 7, respectively. Postnatal day 3, 5, and 7 primary myocyte preparations were co-stained for IRX4 (B, F, J) and cTnT (C, G, K). Alexa fluor 488 and -568 channels were merged to illustrate the intracellular localization of Irx4 protein in primary myocytes (D, H, L). (M) Graph depicting the average pixel intensity within nuclei. Errors represent standard deviation. n=60. ****P < 0.0001. Arrowheads in F point to nuclei that are positive for Irx4 expression. Abbreviations: P, postnatal. Scale bars, 25μm.

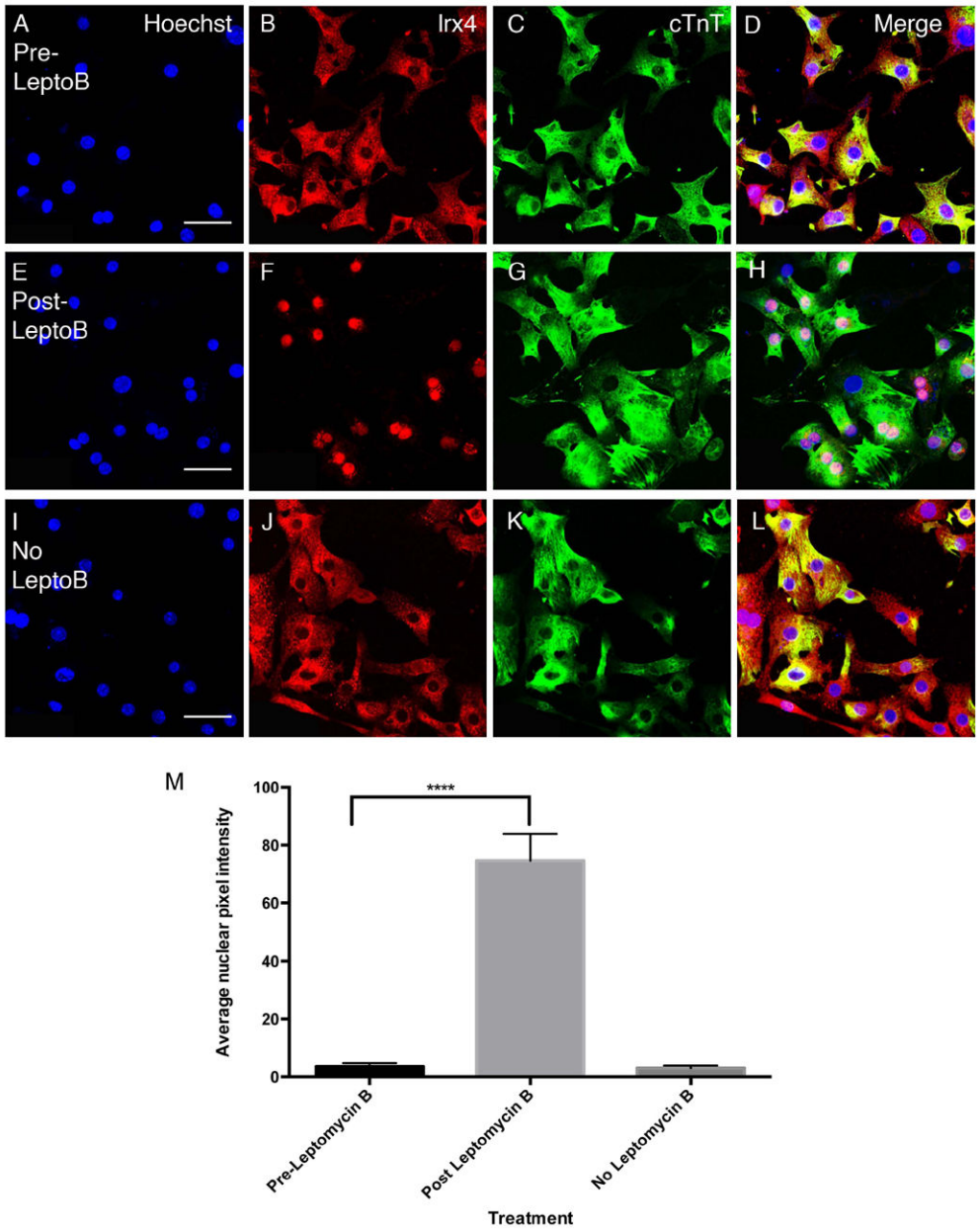

Figure 7. The CRM1 pathway is responsible for IRX4 nuclear export

Confocal microscopy of E12.5 cardiomyocyte explant cultures. The panels represent a single focal plane. (A, E, I) Hoechst stain, (B, F, J) IRX4 stain, and (C, G, K) cTnT stain of primary myocyte preparations before, after, and omitting Leptomycin B treatment, respectively. (D, H, L) Alexa fluor 488 and -568 channels were merged. (M) Graph illustrating the average pixel intensity detected within nuclei. Errors represent standard deviation. n=60. ****P < 0.0001. Abbreviations: LeptoB, Leptomycin B. Scale bars, 50μm.